A diffusive model for evaluating thickness of bedload layer

Cheng, Nian-Sheng

2003

Cheng, N. S. (2003) A diffusive model for evaluating thickness of bedload layer. Advances in Water Resources, 26(8), 875-882.

https://hdl.handle.net/10356/94298

https://doi.org/10.1016/S0309-1708(03)00062-9

A diffusive model for evaluating thickness of bedload layer

*Nian-Sheng Cheng**

School of Civil and Structural Engineering, College of Engineering, Nanyang Technological University, Nanyang Avenue, Singapore 639798, Singapore

E-mail address: cnscheng@ntu.edu.sg (N.-S. Cheng).
** Tel.: +65-6790-6936; fax: +65-6791-0676.*

Abstract

The thickness of the bedload layer is a crucial parameter for evaluating sediment transport rates in open channel flow, but it is often determined empirically. Based on the concept of the hydrodynamic diffusion related to particle–particle interactions, an analytical model is proposed in this study for computing the thickness of the bedload layer. The coefficient of diffusion is assumed to be associated with the momentum transfer induced by the random particle motion and thus can be derived from the shear-induced particle stress. The analytical result shows that the ratio of the bedload thickness to the particle diameter depends on the dimensionless particle diameter and dimensionless bed shear stress. Differences are also examined between the present study and a few empirical formulas that are derived from experimental results for limited bed conditions.

Keywords: Bedload layer; Hydrodynamic diffusion; Sediment transport; Bed shear stress; Two-phase flow

1. Introduction

The transport of sediment particles in open channel flows is usually divided into bedload and suspended load. This categorization is found to be convenient for conducting relevant studies on sediment transport because the underlying mechanism of bedload transport is different from that of suspended load. It is generally believed that turbulence eddies have significant effects on the motion of suspended particles. Turbulence also plays an important role in the incipient motion of bed sediment particles. However, once moving, the particles of bedload would experience continuous contacts with the bed in the mode of rolling, sliding or saltation. This implies that hydrodynamic interactions among the particles would have a commanding influence on bedload transport.

Moreover, for particles moving typically in the mode of saltation, their trajectories follow the ballistic path [1]. Therefore, the thickness of the bedload layer may be defined as the saltation height of particles, which is of the order of the particle size. This thickness is usually required to formulate the bedload transport rate analytically. Einstein [2] simply took the thickness to be two particle diameters, independent of flow conditions. His assumption is acceptable only on qualitative grounds, in comparison with several

subsequent studies, which show either experimentally or numerically that the thickness is closely related to characteristics of flow and particles.

Experimental observations of the trajectories of bed particles using photographic techniques have been performed by several researchers [1,3–7]. On the other hand, a few attempts have also been made to numerically simulate motion of the bed particles by considering various forces exerted on a saltating particle (e.g., [7,8]). These studies have resulted in several formulations for relating the thickness of the bedload layer to parameters associated with flow and particles. For example, Lee and Hsu [4] obtained the following correlation equation from their measurements of the average particle saltation height, δ:

$$\frac{\delta}{D} = 14.27(\tau_* - \tau_{*c})^{0.575} \tag{1}$$

where $\tau_* = u_*^2/[(s-1)gD]$ is the Shields number or dimensionless shear stress; $\tau_{*c} = u_{*c}^2/[(s-1)gD]$ the dimensionless critical shear stress; u_*, the shear velocity; u_{*c} the critical shear velocity for the threshold condition of initial particle motion; D the particle diameter; s the specific gravity of particles; and g the gravitational acceleration. Hu and Hui's experimental results suggested that the relative thickness, δ/D, was related to the specific gravity of particles, the dimensionless bed shear stress, and the condition of the bed surface [6]. Their empirical relationships include

$$\frac{\delta}{D} = 3.67 s^{1.05} \tau_*^{0.82} \tag{2}$$

for smooth beds, and

$$\frac{\delta}{D} = 1.78 s^{0.86} \tau_*^{0.69} \tag{3}$$

for rough beds.

Similar correlations can also be obtained based on numerically generated trajectories for the bedload particles. For example, van Rijn's simulation led to the following expression [8]:

$$\frac{\delta}{D} = 0.3 \left(\frac{u_*^2}{u_{*c}^2} - 1 \right)^{0.5} D_*^{0.7} \tag{4}$$

where $D_* = D[((s-1)\rho^2)/\mu^2\,]^{1/3}$ is the dimensionless particle diameter, ρ the density of fluid, and μ the dynamic viscosity of fluid. The format of correlation used by Lee et al.

[7] is the same as Eq. (4) but with the different coefficient and exponents. It reads

$$\frac{\delta}{D} = 0.088\left(\frac{u_*^2}{u_{*c}^2} - 1\right)^{0.71} D_*^{0.63} \tag{5}$$

Nomenclature

c	concentration of particles	w_m	settling velocity of the particle–fluid mixture
c_m	maximum concentration of densely packed particles	w_0	settling velocity of a solitary particle in fluid
D	particle diameter	w_r	w_m/w_0 = relative settling velocity
D_*	$[((s-1)\rho^2 g)/\mu^2]^{1/3} D$ = dimensionless particle diameter	z_b	surface elevation of bedload
D_{*m}	$[((\rho_p/\rho_m - 1)\rho_m^2 g)/\mu_m^2]^{1/3} D$ = dimensionless particle diameter for the particle–fluid mixture	z_c	elevation of the interface between the bedload and stationary bed
du_m/dy	velocity gradient of the bulk flow	z_0	initial elevation of the bed surface in still water
E	diffusion coefficient	α	coefficient
E_*	dimensionless diffusion coefficient	β	constant
F_d	upward hydrodynamic diffusive flux	δ	average thickness of the bedload layer or saltation height of particles
F_s	downward flux of the particles	Δ	$\rho_p/\rho - 1 = s - 1$
G	average gap among neighbouring particles	μ	dynamic viscosity of fluid
g	gravitational acceleration	μ_m	effective viscosity of the particle–fluid mixture
n	exponent	μ_r	μ_m/μ = relative viscosity
R_m	$\rho_m w_m D/\mu_m$ = settling Reynolds number for the particle–fluid mixture	ρ	density of fluid
R_0	$\rho w_0 D/\mu$ = settling Reynolds number	ρ_m	$\rho_p c + \rho(1-c)$ = density of the particle–fluid mixture
s	ρ_p/ρ = specific gravity of particles	ρ_p	density of particles
u_*	shear velocity	τ_b	bed shear stress
u_{*c}	critical shear velocity for incipient sediment motion	τ_p	particle-related shear stress
u_m	velocity of the particle–fluid mixture	τ_*	$u_*^2/[(s-1)gD]$ = Shields number or dimensionless shear stress
V	a finite volume	τ_{*c}	$u_{*c}^2/[(s-1)gD]$ = critical Shields number for incipient sediment motion

It can be seen that obvious discrepancies exist among the above equations. This is not surprising due to two main reasons. First, the bed conditions for the different experimental observations are inconsistent. For example, the boundaries employed by Hu and Hui [6] were either smooth or rough but movable, while those used in [4,7] comprised of particles fixed on flat channel bottoms. The different bed conditions may have different effects on the particle saltation.

The second reason is that different forces were involved in the numerical simulations conducted by different investigators (e.g., [7,8]). Due to complex flow conditions near the bed, it is not clear so far what kinds of forces should be considered for the simulation and how the force-related coefficients such as the drag coefficient can be evaluated precisely.

In addition to the above empirical relationships, it seems that no analytical results are available in the literature for determining the thickness of the bedload layer. This paper

attempts to present a framework for an analysis that can be performed using a diffusive model. This study was partially motivated by recent studies on the hydrodynamic diffusion conducted largely in chemical engineering, which indicate that the hydrodynamic particle–particle interaction can effectively be described as a diffusive process [9].

Depending on flow conditions and properties of particles, different diffusion mechanisms can be identified associated with transport of particles in fluids. For colloidal particles, the diffusion caused by the thermal effect is significant, leading to the Brownian motion of small particles. If the ambient turbulence is intensive, the diffusive characteristics of particles are largely associated with turbulent eddies. For certain conditions, the turbulent diffusion can be considered solely dependent on the momentum transfer of fluid. It is with this assumption that the well-known Rouse equation is derived for computing the concentration profile of suspended particles in open channel flows. The hydrodynamic diffusion refers to the phenomenon that a particle executes a random walk solely because of the particle–particle interaction. It is not due to the thermal effect and can take place even at very small particle Reynolds numbers, implying that it is not caused either by the fluid inertia. This phenomenon has been confirmed experimentally [9–11]. It is also noted that the concept of the hydrodynamic diffusion has successfully been applied to several two-phase flow problems, such as, variations in the effective viscosity of sheared suspensions and resuspension of particles caused by viscous shear stresses [11,12]. Among the three diffusion processes, the hydrodynamic diffusion may be the most essential for the bedload transport. First, this is because the bed particles are usually non-colloidal, implying that the thermal effect is negligible. The second reason is that even though the bedload transport is definitely affected by turbulence, such effects are expected to be insignificant in comparison to the hydrodynamic particle–particle interactions, in particular, for high sediment transport rates. Interesting evidence in this respect may date back to Francis [1], who demonstrated that the particle saltation could even occur in the absence of turbulence, i.e., in laminar flow.

In this study, as a first approximation, the turbulence effect on bedload transport is neglected. A diffusive model is therefore proposed for describing the particle flux perpendicular to the flow direction, which enables evaluation of the thickness of the bedload layer. The preliminary results obtained are presented in comparison with the previous empirical correlations.

2. Theory

Consider a bedload layer as sketched in Fig. 1. The initial elevation of the bed surface is z_0. For a certain flow condition, an equilibrium interface at the elevation, z_c, can be identified between the bedload of which the particles are moving and the stationary particles beneath the bedload. The thickness of the bedload layer, δ, is therefore equal to the distance from the top of the bedload to the interface, i.e., $(z_b - z_c)$. If the bed particles move typically in the mode of saltation, then the bedload thickness can be easily measured as the saltation height.

The bed particles, once saltating, will fall down to the bed because of the gravitational effect. The downward flux of the particles, F_s, can be related to the settling velocity, w_m, and the local concentration of the particles, c:

$$F_s = w_m c \tag{6}$$

where the subscript m indicates the settling velocity occurring in the particle–fluid mixture. This settling velocity can be further expressed in terms of the settling velocity, w_0, under a very dilute condition,

$$w_m = w_r w_0 \tag{7}$$

where w_r is the relative settling velocity depending on the concentration as well as the properties of the particle. Usually, it takes the following form:

$$w_r = (1 - c)^n \tag{8}$$

where n can be empirically related to the dimensionless particle diameter, D_*, or the settling Reynolds number [13]. Instead, a generalized approach for evaluating w_r is used in this study, as detailed in the subsequent section.

Besides the gravity-driven particle flux, the upward hydrodynamic diffusive flux is

$$F_d = -E\frac{dc}{dy} \tag{9}$$

where E is the diffusion coefficient. It is this diffusive flux that causes the bed dilatation in the vertical direction, as sketched in Fig. 1. At equilibrium, the net flux of the particle is zero. Equating Eq. (6) and Eq. (9) yields

$$w_r w_0 c = -E\frac{dc}{dz} \tag{10}$$

Note that the particle concentration for bedload is zero above $z = z_b$, and approaches the maximum value, c_m, for the condition of the densely packed particles below $z = z_c$. Integrating (10) from $z = z_c$ to $z = z_b$ for the bedload layer yields

$$\int_{c_m}^{0} -\frac{E}{w_r c}dc = \int_{z_c}^{z_b} w_0\,dz = w_0(z_b - z_c) \tag{11}$$

Therefore, the elevation difference, (z_b - z_c), i.e., the thickness of the bedload layer δ can be expressed as

$$\delta = \frac{1}{w_0}\int_0^{c_m} \frac{E}{cw_r}\mathrm{d}c \tag{12}$$

From Eq. (12), it follows that the thickness can be analytically evaluated provided that detailed information on the diffusivity E and the relative settling velocity w_r is available.

2.1 Hydrodynamic diffusivity, E

The previous studies show that the hydrodynamic diffusivity E in shear flows is generally proportional to the bulk velocity gradient and the square of the particle diameter [10]:

$$E = E_* D^2 \frac{\mathrm{d}u_m}{\mathrm{d}y} \tag{13}$$

where $\mathrm{d}u_m/\mathrm{d}y$ is the velocity gradient of the bulk flow; u_m the velocity of the mixture; and E_*. the dimensionless diffusivity depending on the particle concentration. The E_*-value deduced from experimental measurements generally increases with increasing particle concentration. However, a general formulation of such a relationship is not yet available.

Alternatively, the diffusivity is assumed in this study to be equivalent to that associated with the momentum transfer induced by the random particle motion. Such an assumption was used previously to investigate concentration profiles of suspended sediment [13]. For example, for deriving the Rouse equation, the diffusion coefficient is expressed in terms of the shear stress distribution according to the linear law and the velocity gradient according to the log-law. Similarly, the diffusivity herein can be related to the particle-related shear stress, τ_p, and the velocity gradient of the bulk flow, $\mathrm{d}u_m/\mathrm{d}y$:

$$E = \frac{\tau_p}{\rho_p \frac{\mathrm{d}u_m}{\mathrm{d}y}} \tag{14}$$

where ρ_p is the density of particles.

The particle shear stress, in general, may comprise three components contributed by the presence of particles, random motion of particles, and inter-particle collision, respectively [14]. When particles are simply present in a fluid, even without relative motion among them, the rheological property of the fluid is modified. On the other hand, the random motion and collision effect lead to 'turbulent' component of the particle shear stress. If this 'turbulent' component is predominant, the particle shear stress can be derived as

$$\tau_p = \alpha \rho_p \left(\frac{D^2}{G} \frac{du_m}{dy} \right)^2 \quad (15)$$

where G is the average gap among neighbouring particles and α = coefficient. Mih [15] reported that α = 0.0122–0.056, generally varying with the coefficient of restitution. The latter can be measured as the ratio of the incident speed to the rebound speed for a vertical bounce of a sphere off an immovable boundary. Eq. (15) was first derived by Bagnold [16], who found that α = 0.0128 for spheres made of wax and lead stearate. Other similar formulations can also be found in [15,17].

Substituting Eq. (15) into Eq. (14) yields

$$E = \alpha \frac{D^4}{G^2} \frac{du_m}{dy} \quad (16)$$

Comparing Eq. (13) to Eq. (16) leads to

$$E_* = \alpha \left(\frac{D}{G} \right)^2 \quad (17)$$

The average gap among neighbouring particles can be determined using the following approach. Consider a certain amount of particles dispersed randomly in a fluid, which yields a volumetric concentration, c. On average, it is assumed that a single particle can be enclosed in a finite volume, V, so that the ratio of the particle volume, $\pi D^3/6$, to V is equal to the concentration, i.e.

$$\frac{\pi D^3/6}{V} = c \quad (18)$$

With Eq. (18), if the volume V is spherical, then its diameter is found to be $Dc^{-1/3}$, which can be considered as the average distance between the centres of two neighbouring particles. Therefore, the average gap G is equal to

$$G = Dc^{-1/3} - D \quad (19)$$

It is noted that Eq. (19) is different from that derived previously by Bagnold [16] for the linear concentration, the latter being sensitive to the particle packing configuration or the maximum particle concentration. Substituting Eq. (19) into Eq. (17) leads to

$$E_* = \alpha(c^{-1/3} - 1)^{-2} \tag{20}$$

With G given by Eq. (19) and the experimental data from [15], one can find that the α-value varies from 0.06 to 0.19.

Furthermore, note that

$$\frac{\mathrm{d}u_\mathrm{m}}{\mathrm{d}y} = \frac{\tau_\mathrm{b}}{\mu_\mathrm{m}} \tag{21}$$

where τ_b is the bed shear stress; $\mu_m = \mu_r\mu$ is the effective viscosity of the mixture; and μ_r the relative viscosity. Substituting Eq. (21) into Eq. (16), after manipulation, yields

$$E = E_* \frac{D_*^3 \tau_*}{\mu_\mathrm{r}} \frac{\mu}{\rho} \tag{22}$$

2.2 Relative viscosity, μ_r

Many empirical formulas are available in the literature for computing the relative viscosity. Their predictions differ in particular for high concentrations. Cheng and Law [18] found that these formulas could be represented well by the following exponential function:

$$\mu_\mathrm{r} = \exp\left[\frac{2.5}{\beta}\left(\frac{1}{(1-c)^\beta} - 1\right)\right] \tag{23}$$

where β is a constant. By comparing Eq. (23) with several empirical relationships, it is found that b varies from 1.0 to 3.9.

2.3 Relative settling velocity, w_r

For the particle–fluid mixture, the settling Reynolds number can be defined as

$$R_\mathrm{m} = \frac{\rho_\mathrm{m} w_\mathrm{m} D}{\mu_\mathrm{m}} \tag{24}$$

where $\rho_m = \rho_p c + \rho(1-c) = (1 + c\Delta)\rho$ is the density of the mixture, and $\Delta = \rho_P/\rho - 1 = $ q — 1. If the particle concentration is vanishingly small, R_m reduces to R_0 *(= $\rho w_0 D/\mu$).* With R_m and R_0, the relative settling velocity w_r can be expressed as

$$w_\mathrm{r} = \frac{\mu_\mathrm{m}}{\mu}\frac{\rho}{\rho_\mathrm{m}}\frac{R_\mathrm{m}}{R_0} = \frac{\mu_\mathrm{r}}{1 + c\Delta}\frac{R_\mathrm{m}}{R_0} \tag{25}$$

Generally, the settling Reynolds number R_0 is a function of the dimensionless particle diameter, D_*. For natural sediment particles, this function can be formulated as [19]:

$$R_0 = \left(\sqrt{2.5 + 1.2D_*^2} - 5\right)^{1.5} \tag{26}$$

As an approximation, Eq. (26) can be further applied to the particle–fluid mixture, yielding

$$R_{\mathrm{m}} = \left(\sqrt{2.5 + 1.2D_{*\mathrm{m}}^2} - 5\right)^{1.5} \tag{27}$$

where $D_{*\mathrm{m}}$ is associated with the properties of the mixture,

$$D_{*\mathrm{m}} = \left[\frac{(\rho_{\mathrm{p}}/\rho_{\mathrm{m}} - 1)\rho_{\mathrm{m}}^2 g}{\mu_{\mathrm{m}}^2}\right]^{1/3} D \tag{28}$$

Eq. (28) can be further rewritten in the following form so that $D_{*\mathrm{m}}$ can be related to D*:

$$D_{*\mathrm{m}} = D_*(1-c)^{1/3}(1+c\Delta)^{1/3}\mu_{\mathrm{r}}^{-2/3} \tag{29}$$

With Eqs. (26), (27) and (29), Eq. (25) can be rewritten as

$$w_{\mathrm{r}} = \frac{\mu_{\mathrm{r}}}{1+c\Delta} \times \left(\frac{\sqrt{2.5 + 1.2D_*^2(1-c)^{2/3}(1+c\Delta)^{2/3}\mu_{\mathrm{r}}^{-4/3}} - 5}{\sqrt{2.5 + 1.2D_*^2} - 5}\right)^{1.5} \tag{30}$$

From Eqs. (23) and (30), it follows that the relative settling velocity varies with the concentration, specific gravity, and dimensionless particle diameter.

2.4 Relative thickness of bedload layer

Substituting Eq. (22) into Eq. (12), one can express the relative thickness as

$$\frac{\delta}{D} = \left(\int_0^{c_m} \frac{E_*}{c\mu_r w_r} \mathrm{d}c \right) \frac{D_*^3}{R_0} \tau_* \qquad (31)$$

where E_*,μ_r, and w_r can be evaluated using Eqs. (20), (23) and (30), respectively. An example of the relationships among δ/D, τ_*, and D_* is plotted in Fig. 2, which is computed using Eq. (31) for α = 0.02, β = 2.5, Δ = 1.65 and c_m = 0.6. Here, β is taken as its average [18], while the values of Δ and c_m are assumed only for the case of natural quartz sediments. The value of α is taken by comparing Eq. (31) to Eq. (1), as detailed in the next section.

Furthermore, effects of the parameters, α, β, Δ and c_m, on the computation are illustrated through Figs. 3– 6. In Fig. 3, α varies with a range of 0.005 to 0.5, which covers the value obtained from Mih's data [15] and that inferred from the subsequent comparisons, while the other three parameters are constant, i.e., β = 2.5, Δ = 1.65 and c_m = 0.6. The β-effect is shown in Fig. 4 for α = 0.02, Δ = 1.65 and c_m = 0.6; the Δ-effect in Fig. 5 for α = 0.02, β = 2.5 and c_m = 0.6; and the c_m-effect in Fig. 6 for α = 0.02, β = 2:5, and Δ = 1.65. From Figs. 3–6, it follows that given the constant dimensionless particle diameter, the α-effect on the saltation height is more significant while the Δ-effect can be neglected. In computing the relationships included in Figs. 3–6, D_* is taken to be 50, which is of the same order of those found from the previous experimental studies. However, similar differences can also be observed for other D_* values.

3. Comparisons with previous studies

To the writer's knowledge, very limited experimental data of the thickness of the bedload layer are available in the literature to fully verify the present study. This may be because the photographic technique used for tracing the particle movement applies only to very low rates of sediment transport, which imply few particles saltating over a flat bed. In particular, the flat bed comprised of fixed particles, which is suitable for conducting measurements but not realistic, is often adopted in some experiments (e.g., [4,7]). On the other hand, with increasing bed shear stress, the bedload layer can vary considerably because the mobile sediment bed may develop from the flat bed into bedforms such as ripples and dunes.

In the following, a preliminary comparison is first made between the present study and the previous empirical relationships, i.e., Eqs. (1)–(5). Then, the analytical result is further discussed when comparing to experimental results for the case of sheet flows, in which the bed shear stress is high and particles move in a concentrated near-bed layer without bedforms.

When comparing the computed thickness using Eq. (31) with those obtained from Eqs. (1)–(5), it is found that various combinations of α- and c_m-values can be used in computing the thickness of the bedload layer. For example, Lee and Hsu's formula, Eq. (1), is in reasonable agreement with the present result for α = 0.02 and c_m = 0.6, as shown in Fig. 7. For consistence, the same α- and c_m-values are also used for comparisons with the other formulas. In computing the thickness with Eq. (31), two different D_*-values, 34 and 62, are used, following the range of the experimental data [4]. The critical shear stress that is included in Eqs. (1), (4) and (5) is computed using the following expression:

$$\tau_{*c} = 0.22D_*^{-0.9} + 0.06\exp(-17.77D_*^{-0.9}) \qquad (32)$$

which is given for fitting the Shields diagram [20].

In Fig. 8, Eq. (31) is presented as δ/D against τ_* for comparing with the formulas, Eqs. (2) and (3), obtained by Hu and Hui [6] for smooth and rough beds, respectively. In the computation, the specific gravity is assumed to be 2.65 for the case of quartz sediment, and the dimensionless particle diameter varies from 15 to 90, being the span given in the Hu and Hui's experiments. Fig. 8 shows that the empirical formulas are close to the present study for D_* = 15 but the considerable difference exists for D_* = 90.

Van Rijn's work [8] indicates that both dimensionless parameters, D_* and $(u_*^2/u_{*c}^2 - 1)$, have significant effects on the relative thickness of the bedload layer. This relationship is reproduced, according to Eq. (4), in Fig. 9, which is also superimposed with the corresponding curves computed with Eq. (31). Fig. 9 shows that for D_* = 10 and 100, the relationships, Eqs. (4) and (31), generally agree with each other. However, being distinct from the van Rijn's formulation, the relative thickness computed using the present approach is dependent only on the dimensionless particle diameter if the bed shear stress is very close to its critical value for the incipient sediment motion, i.e.,$\tau_*/\tau_{*c} \rightarrow 1$. The similar phenomenon can also be observed in Fig. 10, which shows the comparison of the curves computed with Eq. (31) and the empirical relationship, Eq. (5), proposed by Lee et al. [7].

On the right-hand side of Eq. (31), it can be seen that the integration is dependent on the concentration distribution within the bedload layer, and the ratio D_*^3/R_0 is only related to the properties of particle and fluid, implying that the relative bedload thickness is proportional to the dimensionless bed shear stress, i.e., $\delta/D \sim \tau_*$. This is different from the empirical relationships, Eqs. (1)–(5), which indicate that the bedload thickness increases slightly slower with increasing bed shear stress, i.e., $\delta/D \sim \tau_*^{(0.575-0.82)}$ if $\tau_* >> \tau_{*c}$. On the other hand, it is noted that for high shear stresses, bedforms disappear and the bed particles move largely in the sheet modes. For this extreme condition, the empirical relationships, Eqs. (1)–(5), may not apply because they are derived based on the experiments for the low transport stage. However, the linear relationship, $\delta/D \sim \tau_*$, seems to be applicable, as reported in [21,22]. Such a relationship was first derived by Wilson [21] based on the consideration of dynamic friction, which yields $\delta/D \sim 10\tau_*$. This simple relationship is also found comparable to the experimental data provided by Sumer et al. [22], who investigated the sheet-flow layer for steady conditions using four kinds of sediment. In the Sumer et al.'s experiment (sediment 3), D = 6.5, c_m = 0.3, and Δ = 0.13. With these values, the computation using Eq. (31) indicates that δ/D is equal to $10\tau_*$ for α = 0.098. Obviously, further investigations should be made to fully verify the present analysis including the determination of the relevant parameters such as α and β that are closely related to the characteristics of sediment particles.

4. Conclusion

Applying the concept of the hydrodynamic diffusion, which is caused by particle–particle interactions, to bedload transport leads to an analytical model that enables the evaluation of the thickness of the bedload layer. The derived result indicates that the bedload thickness is related to the dimensionless particle diameter and dimensionless bed shear stress. The computed bedload thickness is generally comparable to the previous empirical formulas provided that the α-coefficient for determining the dimensionless diffusivity is calibrated.

Being limited to the assumption made, this study may be more applicable to the case of high concentrated bedload transport or sheet flows. However, relevant experimental data are still lacking, which means that detailed comparisons for such cases cannot be made at present.

Further research needs to be done to fully verify and improve the analysis presented herein. In particular, it is essential to know how the α-coefficient can be evaluated precisely. It is noted that the coefficient generally varies with the coefficient of restitution of particles. However, it is not clear that what range of values should be used, for example, for typical sediment particles. On the other hand, the present study can be further improved by considering effects of the near-bed turbulence on the bed particle motion. It would also be compelling to understand how significant the turbulence effect on the thickness of bedload layer could be when compared to the hydrodynamic particle–particle interaction.

References

[1] Francis JRD. Experiments on the motion of solitary grains along the bed of a water-stream. Proc Roy Soc London, Ser A 1973;332(1591):443–71.

[2] Einstein HA. The bed-load function for sediment transportation in open channel flow. United States Department of Agriculture, Washington, DC, Technical Bulletin No. 1026. 1950, 78p.

[3] Abbott JE, Francis JRD. Saltation and suspension trajectories of solid grains in a water stream. Proc Roy Soc London, Ser A 1977;284(1321):225–54.

[4] Lee HY, Hsu IS. Investigation of saltating particle motions. J Hydraul Eng, ASCE 1994;120(7):831–45.

[5] Nino Y. Particle motion in the near wall region of a turbulent open channel flow: implications for bedload transport by saltation and sediment entrainment into suspension. PhD Thesis, University of Illinois at Urbana-Champaign, Urbana, IL. 1995, 370p.

[6] Hu C, Hui Y. Bed-load transport I: mechanical characteristics. J Hydraul Eng, ASCE 1996;122(5):245–54.

[7] Lee HY, Chen YH, You JY, Lin YT. Investigation of continuous bed load saltating process. J Hydraul Eng, ASCE 2000;126(9): 691–700.

[8] van Rijn LC. Sediment transport. Part I: bed load transport. J Hydraul Eng, ASCE 1984;110(10):1431–56.

[9] Eckstein EC, Bailey DG, Shapiro AH. Self-diffusion of particles in shear flow of a suspension. J Fluid Mech 1977;79:191–208.

[10] Leighton D, Acrivos A. The shear-induced migration of particles in concentrated suspensions. J Fluid Mech 1987;181:415–39.

[11] Brady JF. Modeling suspension flows. Liquid–Solid Flows, The 1994 ASME Fluid Engineering Division Summer Meeting. FED 1994;189:11.

[12] Acrivos A, Mauri R, Fan X. Shear-induced resuspension in a Couette device. Int J Multiphase Flow 1993;19(5):792–802.

[13] Raudkivi AJ. Loose boundary hydraulics. Rotterdam: AA Balkema; 1998. p. 496.

[14] Hwang GJ, Shen HH. Modeling the solid phase stress in a fluid– solid mixture. Int J Multiphase Flow 1989;15(2):257–68.

[15] Mih WC. High concentration granular shear flow. J Hydraul Res 1999;37(2):229–48.

[16] Bagnold RA. Experiments on a gravity-free dispersion of large solid spheres in a Newtonian fluid under shear. Proc Roy Soc London 1954;A225:49–63.

[17] Shen H, Ackermann NL. Constitutive relationships for fluid–solid mixtures. J Eng Mech, ASCE 1982;108(5):748–63.

[18] Cheng NS, Law AWK. Exponential formula for computing effective viscosity. Powder Technol 2003;129(1–3):156–60.

[19] Cheng NS. Simplified settling velocity formula for sediment particle. J Hydraul Eng, ASCE 1997;123(2):149–52.

[20] Brownlli WR. Prediction of flow depth and sediment discharge in open channels. Rep. N-KH-R-43A, Keck Lab of Hydr and Water Resour, California Institute of Technology, Pasadena, California, USA. 1981, 232p.

[21] Wilson KC. Analysis of bed-load motion at high shear stress. J Hydraul Eng, ASCE 1987;113(1):97–103.

[22] Sumer BM, Kozakiewicz A, Fredsoe J, Deigaard R. Velocity and concentration profiles in sheet-flow layer of movable bed. J Hydraul Eng, ASCE 1996;122(10):549–58.

List of Figures

Fig. 1 Definition sketch for thickness of bedload layer.

Fig. 2 Variations of relative bedload thickness with dimensionless particle diameter and dimensionless bed shear stress.

Fig. 3 Effect of α on relative bedload thickness.

Fig. 4 Effect of β on relative bedload thickness.

Fig. 5 Effect of specific gravity on relative bedload thickness.

Fig. 6 Effect of maximum particle concentration on relative bedload thickness.

Fig. 7 Comparison with Lee and Hsu's empirical formula.

Fig. 8 Comparison with Hu and Hui's correlations.

Fig. 9 Comparison with van Rijn's simulated results.

Fig. 10 Comparison with Lee et al.'s empirical formula.

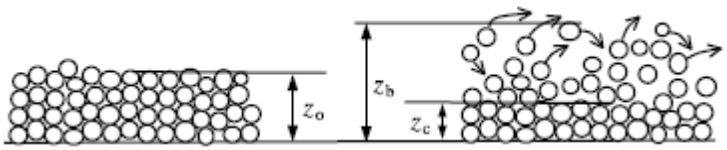

Fig. 1

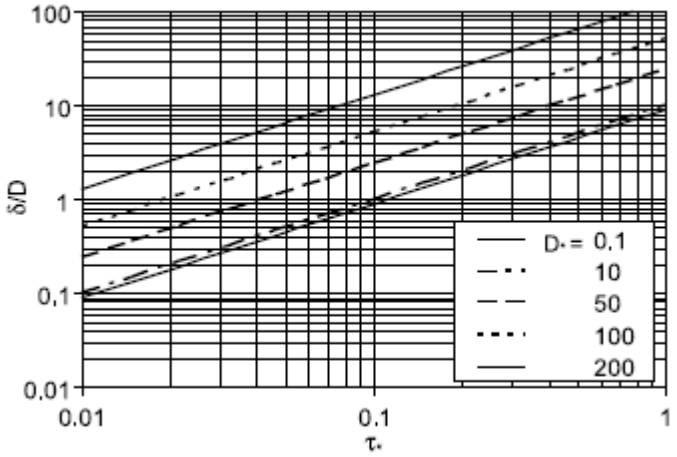

Fig. 2

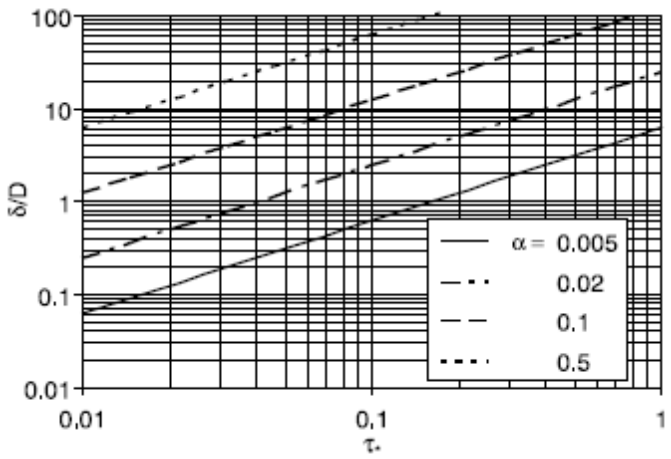

Fig. 3

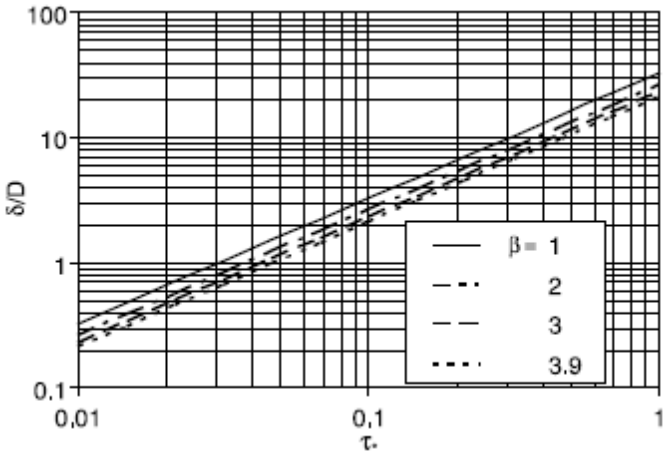

Fig. 4

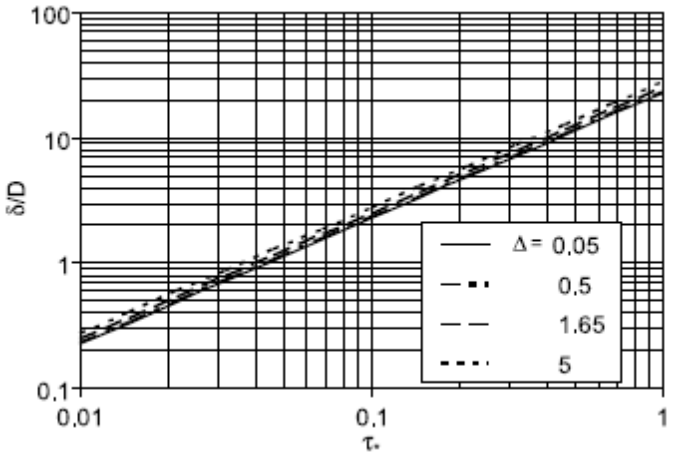

Fig. 5

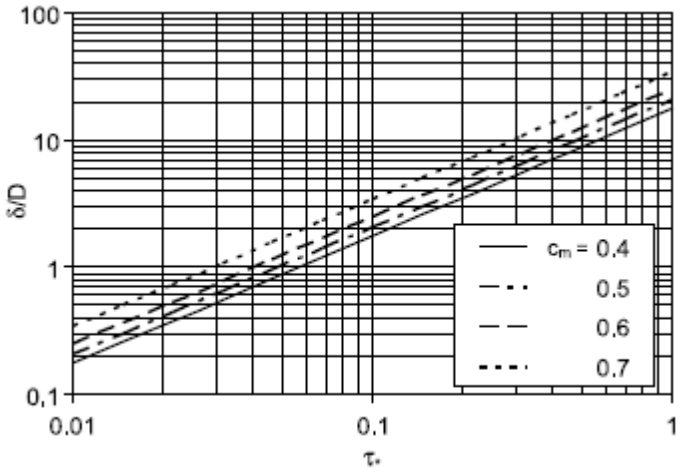

Fig. 6

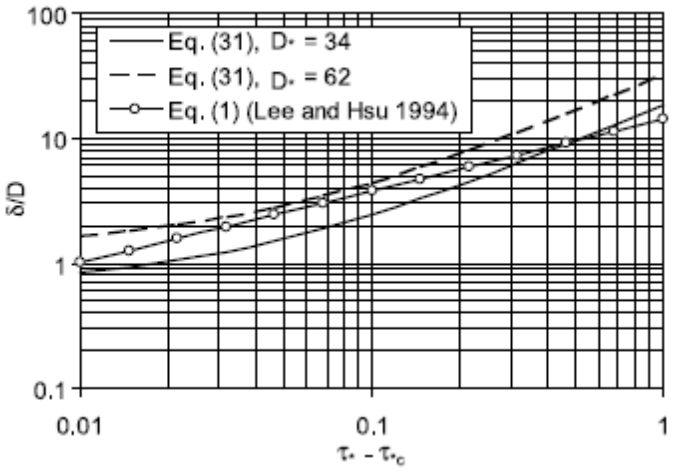

Fig. 7

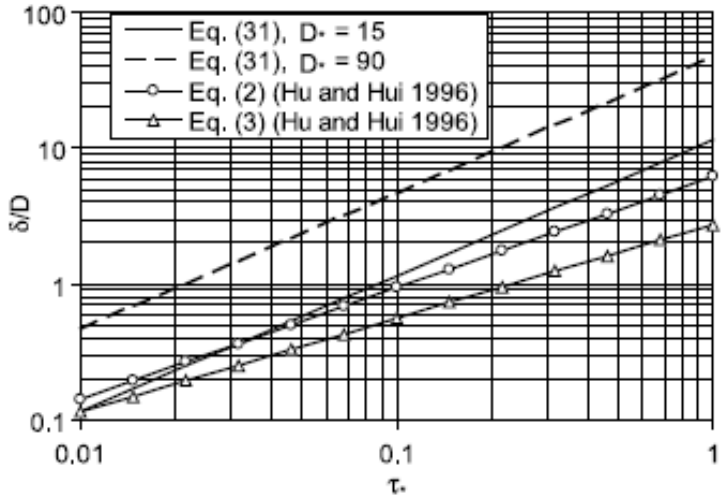
Eq. (31), D* = 15
Eq. (31), D* = 90
Eq. (2) (Hu and Hui 1996)
Eq. (3) (Hu and Hui 1996)
100
10
1
0.1
δ/D
0.01
0.1
1
τ*

Fig. 8

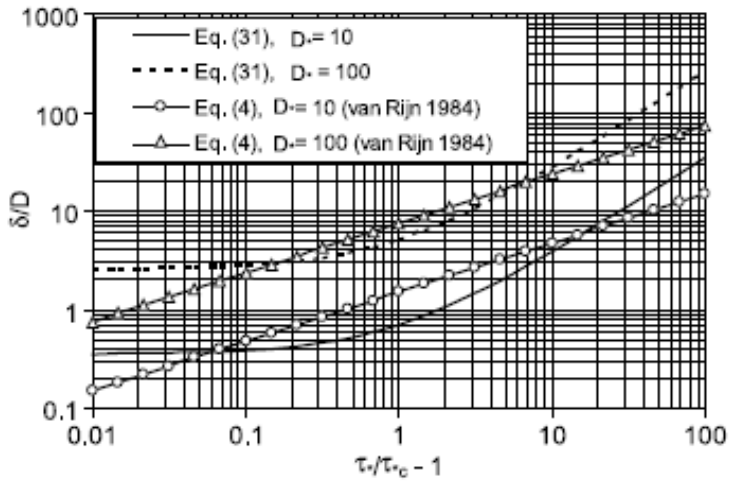
Eq. (31), D*= 10
Eq. (31), D* = 100
Eq. (4), D*= 10 (van Rijn 1984)
Eq. (4), D*= 100 (van Rijn 1984)
δ/D
1000
100
10
1
0.1
0.01
0.1
1
10
100
τ*/τ*c - 1

Fig. 9

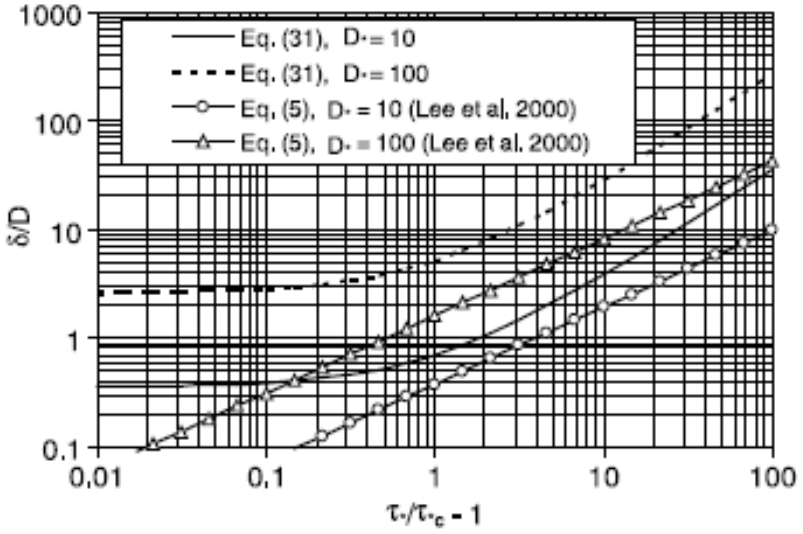
Eq. (31), D* = 10
Eq. (31), D* = 100
Eq. (5), D* = 10 (Lee et al, 2000)
Eq. (5), D* = 100 (Lee et al. 2000)
δ/D
1000
100
10
1
0.1
0,01
0,1
1
10
100
τ*/τ*c - 1

Fig. 10